Journal of Physical Science and Application 8 (2) (2018) 28-42
doi: 10.17265/2159-5348/2018.02.005

Ultra-Modified Control Algorithms for Matrix Converter in Wind Energy System

Kotb B. Tawfiq, A. M. Mansour and E. E. EL-Kholy
Department of Electrical Engineering, Faculty of Engineering, Menoufia University 11341, Egypt

Abstract: This paper proposes an ultra-modified SSA (symmetric sequence algorithm) of space vector modulation of MC (matrix converter). The ultra-modified technique improves the drawbacks of the modified one where it provides a reduction of the total harmonic distortion for both output voltage and current. Also this paper proposes a modified feed forward controller of the MC with indirect space vector modulation. The modified feed forward provides a solution for the change in the output voltage due to change in wind speed, where it provides a constant output voltage with constant frequency even if the wind speed changed. Some of the advantages of MC are introduced in this paper. These advantages represented in the output frequency of MC which may be greater than the input frequency, controlling rms value of the output voltage and the ability to control the IDF (input displacement factor). At the end of this paper simulation and experimental results are introduced which give a precise proof to the proposed algorithms.

Key words: MC, SSA, modifed feed forward control, WECS (wind energy conversion system).

1. Introduction

A lot of exertion is being made to create power from renewable sources of energy. The significant favorable advantage of utilizing renewable sources is absence of harmful emissions. Wind generators have been generally utilized in autonomous systems. AC can be directly converted to AC with different voltage rms value and different frequency by using a MC (matrix converter) without using any DC link and this is the bold feature of MC over rectifier-inverter converter, so MC can be considered an emerging alternative to the conventional rectifier-inverter converter. Independent control on the output voltage magnitude and frequency can be provided by utilizing a MC. In addition to control the phase angle between input voltage and input current and unity IDF (input displacement factor) can be achieved. However, this topology does not take its proper place in the industry so far [1, 2]. There are many space vector modulation algorithms. In this paper an ultra-modified SSA is proposed. This method has lower THD of voltage compared to conventionaland modified SSA, so the size of the required filter is reduced. Also a modified feed forward controller of the MC with indirect space vector modulation will be proposed. The organization of this paper is as follows: In the second part, a short description of WT (Wind Turbine) is introduced, in addition to demonstrate how the wind energy can be ideally caught and changed over to electric energy; in the section three, a short description on operation of a SCIG (Squirrel-Cage Induction Generator) is introduced; in the section four, indirect space vector control of MC is presented a short description of MC is introduced. And indirect space vector control of MC is presented showing how to transform from indirect converter to direct one [3, 4]. MC is used to control load voltage and frequency. In the section five, the ultra-modified SSA is proposed. Next part, modified feed forward control of MC is introduced. Then, describe how to implement the proposed system in the laboratory. Finally, simulation and experimental results for different operating points are displayed.

Corresponding author: Kotb B. Tawfiq, master, engineer, research fields: renewable energy, power electronic and electrical drive.

2. Wind Turbine

The produced mechanical power from turbine is given by Eq. (1). Fig. 1 shows the generated mechanical power with turbine speed.

$$P_m = \frac{1}{2}\rho c_p A_r v_w^3 \quad (1)$$

$$c_p(\lambda,\theta) = 0.73\left(\frac{151}{\lambda_i} - 0.58\theta - 0.002\theta^{2.14} - 13.2e{-}18.4\lambda i\right) \quad (2)$$

$$\lambda_i = \frac{1}{\frac{1}{\lambda - 0.02\theta} - \frac{0.003}{\theta^3+1}} \quad (3)$$

$$\lambda = \frac{\omega_r R_r}{v_w} \quad (4)$$

where, P_m represents generated power, v_w is wind speed in, ρ is air density, A_r rotor area.

3. Squirrel-Cage Induction Generator

IG (induction generator) is suitable in WT as they produce valuable power at different rotor speeds. Fig. 2 shows the equivalent circuit of IG. Reactive power required for IG can be achieved by connecting a capacitor bank across the stator terminals [5, 6].

$$\begin{Bmatrix} V_s^{abc} \\ 0^{abc} \end{Bmatrix} = \begin{bmatrix} r_s^{abc} & 0 \\ 0 & r_r^{abc} \end{bmatrix} \begin{Bmatrix} i_s^{abc} \\ i_r^{abc} \end{Bmatrix} + \frac{d}{dt}\begin{Bmatrix} \lambda_s^{abc} \\ \lambda_r^{abc} \end{Bmatrix} \quad (5)$$

4. Matrix Converter

MC is an AC-AC converter that consists of nine-bidirectional switches which provides a direct connection between the input voltage with the load so MC can be manufactured in a compact form, shown in Fig. 3. MC has the ability of bi-directional power flow, unity IDF can be provided [7]. It has limited input output voltage transfer ratio to 0.866 for sinusoidal input and output waveforms [8, 9]. Because of the lack of switches that allow to the current to flow in both directions, some MC types need more number of switches compared to conventional rectifier-inverter type. Input filters are required to reduce the high frequency harmonics and clamping circuits are needed to protect switches from over voltages due to energy stored in inductive loads. In 1976 Gigi and Pelly [5] introduce the first principle of a MC. The first mathematical form of MC was introduced in 1980 by Venturini and switches are the primary disadvantage of this converter [6].

4.1 Construction of MC

The main structures of MC are: matrix switches, input filter and clamping circuit [10].

4.2 Control of MC

MC consists of nine-bidirectional switches which

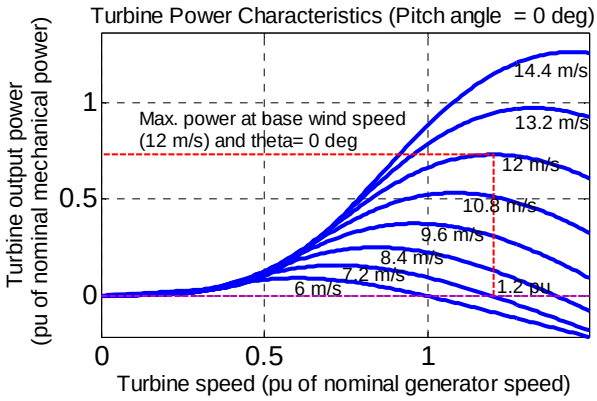

Fig. 1 Mechanical power with turbine speed.

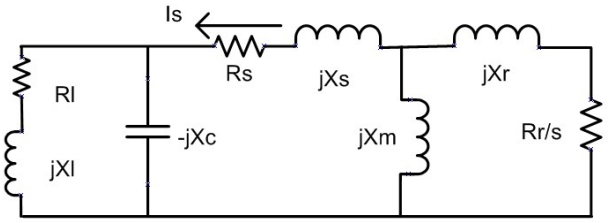

Fig. 2 Equivalent circuit of IG.

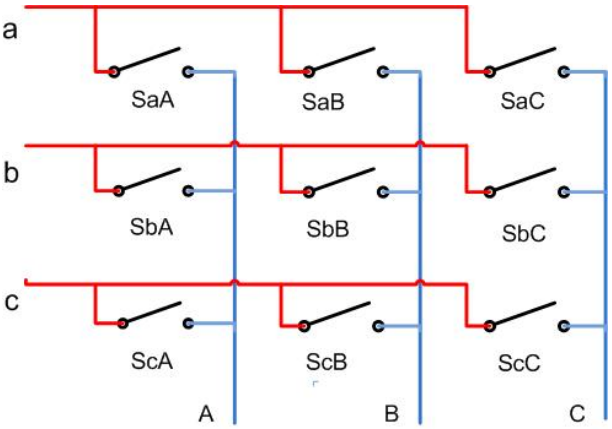

Fig. 3 Direct MC (MC).

allow all input lines to connect to all output lines as shown in Fig. 4. ISVM is the control strategy used in this paper.

4.2.1 Transformation from Indirect MC to Direct MC

ISVM deals with MC as a rectifier-inverter combination with virtual DC link as shown in Fig. 4. Indirect MC consists of two stages, first stage is rectifier based on switches S1-S6, second stage is inverter, which has a standard three phases voltage source topology based on six switches S7-S12 [11].

$$V_{DC} = E * V_{abc},\ V_{ABC} = N * V_{DC},\ V_{ABC} = \mathrm{N} * \mathrm{E} * V_{abc},\ \mathrm{K} = \mathrm{N} * \mathrm{E} \quad (6)$$

$$E = \begin{bmatrix} S_1 & S_3 & S_5 \\ S_2 & S_4 & S_6 \end{bmatrix},\ N = \begin{bmatrix} S_7 & S_8 \\ S_9 & S_{10} \\ S_{11} & S_{12} \end{bmatrix},\ K = \begin{bmatrix} S_{aA} & S_{bA} & S_{cA} \\ S_{aB} & S_{bB} & S_{cB} \\ S_{aC} & S_{bC} & S_{cC} \end{bmatrix} \quad (7)$$

$$\begin{bmatrix} S_{aA} & S_{bA} & S_{cA} \\ S_{aB} & S_{bB} & S_{cB} \\ S_{aC} & S_{bC} & S_{cC} \end{bmatrix} = \begin{bmatrix} S_7 & S_8 \\ S_9 & S_{10} \\ S_{11} & S_{12} \end{bmatrix} \begin{bmatrix} S_1 & S_3 & S_5 \\ S_2 & S_4 & S_6 \end{bmatrix} \quad (8)$$

space vector of the inverter and rectifier can be decoupled to control direct MC [12]. As in Eq. (9) the output phases can be compounded by the product and sum of input phases through rectifier and inverter switches $S_1 - S_6$ and $S_7 - S_{12}$ respectively. The first row of the matrix in Eq. (9) shows how to obtain output phase A from input phases *a*, *b* and *c* for direct MC using ISVM as in Fig. 5 [13, 14].

$$\begin{bmatrix} V_A \\ V_B \\ V_C \end{bmatrix} = \begin{bmatrix} S_7 & S_8 \\ S_9 & S_{10} \\ S_{11} & S_{12} \end{bmatrix} \begin{bmatrix} S_1 & S_3 & S_5 \\ S_2 & S_4 & S_6 \end{bmatrix} \begin{bmatrix} v_a \\ v_b \\ v_c \end{bmatrix} \quad (9)$$

$$\begin{bmatrix} V_A \\ V_B \\ V_C \end{bmatrix} = \begin{bmatrix} S_7S_1 + S_8S_2 & S_7S_3 + S_8S_4 & S_7S_5 + S_8S_6 \\ S_9S_1 + S_{10}S_2 & S_9S_3 + S_{10}S_4 & S_9S_5 + S_{10}S_6 \\ S_{11}S_1 + S_{12}S_2 & S_{11}S_3 + S_{12}S_4 & S_{11}S_5 + S_{12}S_6 \end{bmatrix} * \begin{bmatrix} v_a \\ v_b \\ v_c \end{bmatrix} \quad (10)$$

4.2.2 CSR (Current Source Rectifier)

CSR consists of six switches S1-S6, as shown in Fig. 6. Rectifier has to generate constant DC voltage from three phase input voltage.

$$\begin{bmatrix} V_{DC}^{+} \\ V_{DC}^{-} \end{bmatrix} = \begin{bmatrix} S_1 & S_3 & S_5 \\ S_2 & S_4 & S_6 \end{bmatrix} \begin{bmatrix} V_a \\ V_b \\ V_c \end{bmatrix} \quad (11)$$

$$\begin{bmatrix} I_a \\ I_b \\ I_c \end{bmatrix} = \begin{bmatrix} S_1 & S_2 \\ S_3 & S_4 \\ S_5 & S_6 \end{bmatrix}^T \begin{bmatrix} I_p \\ I_n \end{bmatrix} \quad (12)$$

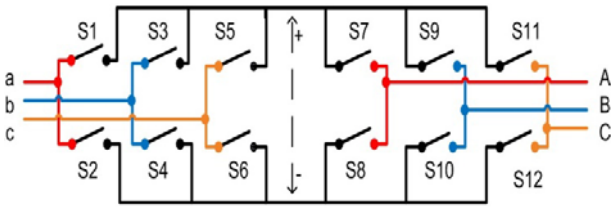

Fig. 4 Indirect MC.

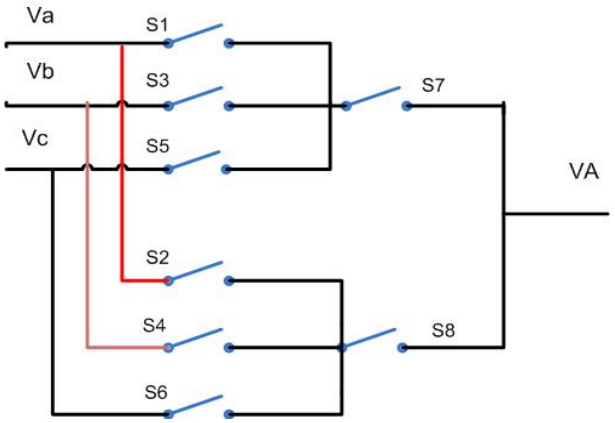

Fig. 5 Transformation from indirect MC to direct one in phase A.

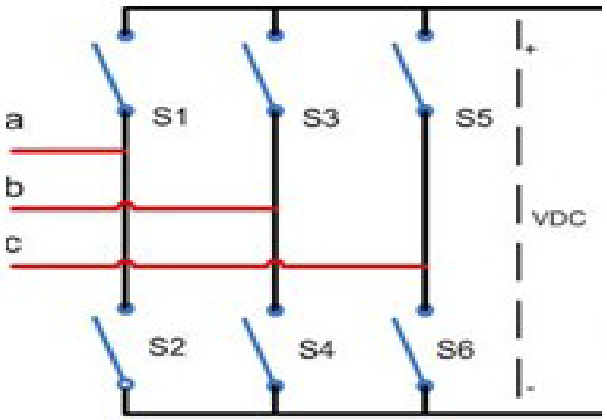

Fig. 6 Current source rectifier.

$$I_{IN} = \frac{2}{3}(I_a + a.I_b + a^2.I_c) \quad (13)$$

For CSR, there is allowed nine switching states to avoid open circuit. These nine states are divided into six active vectors $\boldsymbol{I_1 - I_6}$ and three zero vectors $\boldsymbol{I_0}$ as shown in Fig. 7a. The current space vector state $\boldsymbol{I_1}$ (a, b) means that input phase a is connected to the positive terminal of the virtual DC link (VDC+) and input phase b is connected to the negative terminal (VDC−). Fig. 7a shows the configuration of the discrete seven space vectors of the input current in a hexagon in a complex plane and the reference input current vector $\boldsymbol{I_{IN}^*}$ within a sector of the input current hexagon [14]. The $\boldsymbol{I_{IN}^*}$ can be obtained by impressing the adjacent active vectors $\boldsymbol{I_\gamma}$ and $\boldsymbol{I_\delta}$ with the duty cycles d_γ and d_δ, respectively, as shown in Fig. 7b.

$$I_{IN}^* = d_\gamma I_\gamma + d_\delta I_\delta + d_{oc} I_0 \quad (14)$$

The active vectors duty cycle can be written as :

$$d_\gamma = m_c \cdot \sin\left(\frac{\pi}{3} - \theta_c\right) \quad (15)$$

$$d_\delta = m_c \cdot \sin(\theta_c) \quad (16)$$

$$d_{0c} = 1 - (d_\gamma + d_\delta) \quad (17)$$

$$m_c = \frac{I_{IN}^*}{I_{DC}} \quad (18)$$

4.2.3 VSI (Voltage Source Inverter)

VSI consists of six switches $S_7 - S_{12}$ as in Fig. 8. The output voltage can be represented as a function of DC input voltage and transfer function of the inverter as in Eq. (14).

$$\begin{bmatrix} V_A \\ V_B \\ V_C \end{bmatrix} = \begin{bmatrix} S_7 & S_8 \\ S_9 & S_{10} \\ S_{11} & S_{12} \end{bmatrix} \begin{bmatrix} \frac{V_{DC}}{2} \\ \frac{-V_{DC}}{2} \end{bmatrix} \quad (19)$$

$$\begin{bmatrix} I_p \\ I_n \end{bmatrix} = \begin{bmatrix} S_7 & S_8 \\ S_9 & S_{10} \\ S_{11} & S_{12} \end{bmatrix}^T \begin{bmatrix} I_A \\ I_B \\ I_C \end{bmatrix} \quad (20)$$

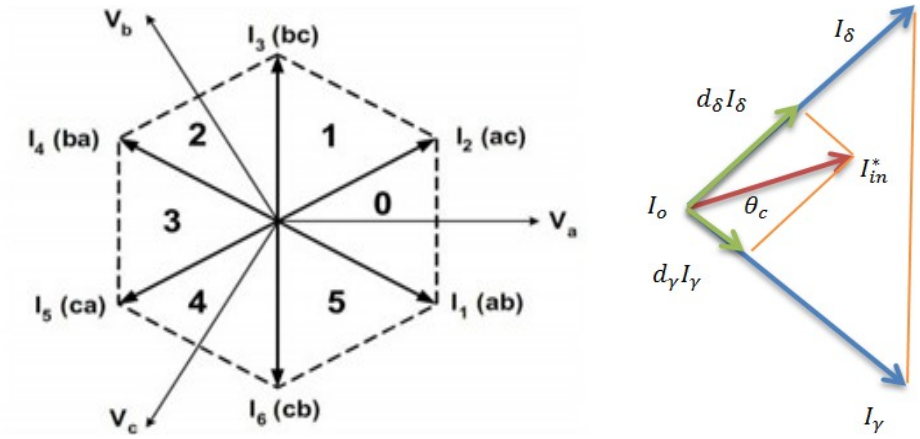

(a) (b)

Fig. 7 (a) Space vector of CSR; (b) Composition of the reference input current.

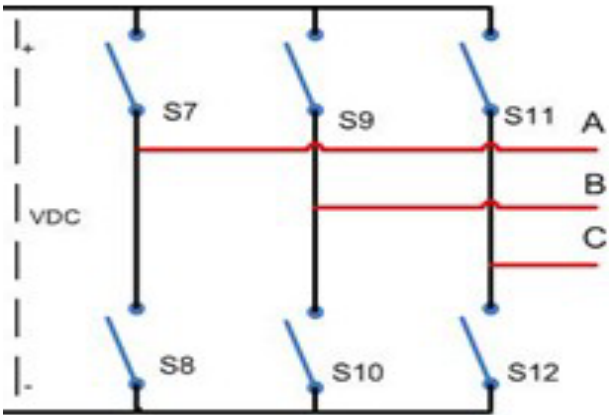

Fig. 8 Voltage source inverter.

The output voltage space vector $\boldsymbol{V_{out}}$ can be expressed as follows:

$$V_{out} = \frac{2}{3}(V_A + a.V_B + a^2.V_C)\,, a = 1 * e^{j120} \quad (21)$$

Inverter switches have only eight allowed states to avoid short on DC link and open in inductive loads. These eight permitted states can be classified into six active output voltage vectors $\boldsymbol{V_1 - V_6}$ and two zero vectors $\boldsymbol{V_z}$. The voltage vector $\boldsymbol{V_1}$ (100) means that $\boldsymbol{V_A}$ is connected to positive terminal of DC link and $\boldsymbol{V_B}$, $\boldsymbol{V_C}$ are connected to negative terminal. Fig. 9a shows the configuration of the discrete space vectors of the output voltage in hexagon. The reference voltage $\boldsymbol{V_O^*}$ can be obtained by a vector sum out of seven discrete voltage vectors, $\boldsymbol{V_1 - V_6}$ and $\boldsymbol{V_z}$. This hexagon can be divided into six sectors. The duty cycles d_α and d_β of active vectors $\boldsymbol{V_\alpha}$ and $\boldsymbol{V_\beta}$, respectively, for the reference vector $\boldsymbol{V_O^*}$ within a sector of the hexagon can be derived from Fig. 9b [15].

$$V_o^* = d_\alpha V_\alpha + d_\beta V_\beta + d_z V_z \quad (22)$$

$$d_\alpha = \frac{T_\alpha}{T_s} = m_v \cdot \sin\left(\frac{\pi}{3} - \theta_v\right) \quad (23)$$

$$d_\beta = \frac{T_\beta}{T_s} = m_v \cdot \sin(\theta_v) \quad (24)$$

$$d_z = \frac{T_z}{T_s} = 1 - (d_\alpha + d_\beta) \quad (25)$$

$$m_v = \frac{\sqrt{3} v_{o,max}}{V_{DC}} \quad (26)$$

5. Symmetric Sequence Algorithm

This section proposes a modified SSA for space vector modulation. The proposed algorithm reduces THD of the output voltage. When the desired output voltage vector of the inverter lies in sector 1 as shown in Fig. 9b. The inverter switches $S_7 - S_{12}$ do not have a state represent this position, so this position can be represented by adjacent vector $\boldsymbol{V_\alpha}$, $\boldsymbol{V_\beta}$ and $\boldsymbol{V_z}$ with duty cycle d_α, d_β and d_z. The main distinction between PWM algorithms that utilize adjacent vectors is zero vector selection, sequence in which the adjacent vectors are applied and splitting of the duty cycle of each adjacent vector [13, 14].

5.1 Conventional SSA

There are many SVM algorithms; one of them is SSA that has low THD as shown in Fig. 10a. During each switching time T_s the duty cycles of each vector $\boldsymbol{V_\alpha}$, $\boldsymbol{V_\beta}$ and $\boldsymbol{V_z}$ (d_α, d_β and d_z) is calculated. In the conventional SSA the duty cycle of vector $\boldsymbol{V_\alpha}$ (d_α) is divided to two equal period, d_β and d_z is also divided to three periods $\frac{d_z}{2}$, $\frac{d_z}{4}$ and $\frac{d_z}{4}$. The sequence in this method is $\boldsymbol{V_z - V_\alpha - V_\beta - V_z - V_\beta - V_\alpha - V_z}$ [13].

5.2 Modified SSA

In Ref. [14] a modified SSA is proposed, the modification in this algorithm is the sequence in which the vectors are applied and the number of division of each duty cycle for each vector. In the modified algorithm the duty cycle of $\boldsymbol{V_\alpha}$ (d_α) is divided to four equal periods, d_β and d_z is also divided

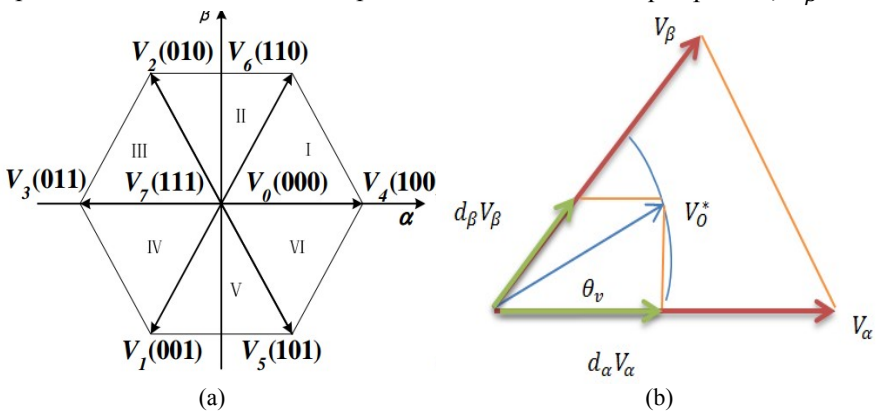

Fig. 9 (a) Hexagon of inverter voltage; (b) Composition of the reference output voltage vector.

to five periods $\frac{d_z}{4}, \frac{d_z}{4}, \frac{d_z}{4}, \frac{d_z}{8}$ and $\frac{d_z}{8}$. The sequence in the proposed algorithm is as follow $\mathbf{V_z} - \boldsymbol{V_\alpha} - \boldsymbol{V_\beta} - \mathbf{V_z} - \mathbf{V_\alpha} - \boldsymbol{V_\beta} - \boldsymbol{V_z} - \boldsymbol{V_\beta} - \boldsymbol{V_\alpha} - \boldsymbol{V_z} - \boldsymbol{V_\beta} - \boldsymbol{V_\alpha} - \boldsymbol{V_z}$ as shown in Fig. 10b.

5.3 Ultra-Modified SSA

This paper proposes an ultra-modified SSA, so that to overcome the drawback of the modified algorithm. In the ultra-modified SSA the duty cycle of $\boldsymbol{V_\alpha}$ (d_α) is divided to six un equal periods $\frac{d_\alpha}{4}, \frac{d_\alpha}{4}, \frac{d_\alpha}{8}, \frac{d_\alpha}{8}, \frac{d_\alpha}{8}$ and $\frac{d_\alpha}{8}$, d_β and d_z is also divided to seven un equal periods $\frac{d_z}{4}, \frac{d_z}{8}, \frac{d_z}{8}, \frac{d_z}{8}, \frac{d_z}{8}, \frac{d_z}{8}$ and $\frac{d_z}{8}$. The sequence in the proposed algorithm is as follows $\boldsymbol{V_z} - \boldsymbol{V_\alpha} - \boldsymbol{V_\beta} - \boldsymbol{V_z} - \boldsymbol{V_\alpha} - \boldsymbol{V_\beta} - \boldsymbol{V_z} - \boldsymbol{V_\alpha} - \boldsymbol{V_\beta} - \boldsymbol{V_z} - \boldsymbol{V_\beta} - \boldsymbol{V\alpha} - \boldsymbol{Vz} - \boldsymbol{V\beta} - \boldsymbol{V\alpha} - \boldsymbol{Vz} - \boldsymbol{V\beta} - \boldsymbol{V\alpha} - \boldsymbol{Vz}$ as in Fig. 10c.

5.4 Implementation of ultra-modified SSA

This part introduces how to implement SVM of VSI with ultra-modified SSA by using MATLAB Simulink. Fig. 11a shows how to transform the reference output voltage into vector angle and amplitude. If the reference output voltage vector of the VSI locates in sector 1 as shown in Fig. 11a the inverter switches $S_7 - S_{12}$ do not have a state represent this position, so this position can be represented by adjacent vector $\boldsymbol{V_\alpha}$, $\boldsymbol{V_\beta}$ and $\boldsymbol{V_z}$ with dutycycle d_α, d_β and d_z. After calculating the duty cycles of each adjacent vectors, every one ask himself how to deal with adjacent vector and the sequence in which these duty cycles are applied to VSI. The answer to this question is modified SSA. Fig. 11b shows the trend of implementation ultra-modified SSA in MATLAB Simulink. The first step is to apply the zero vectors for a time equal to one-fourth its period.

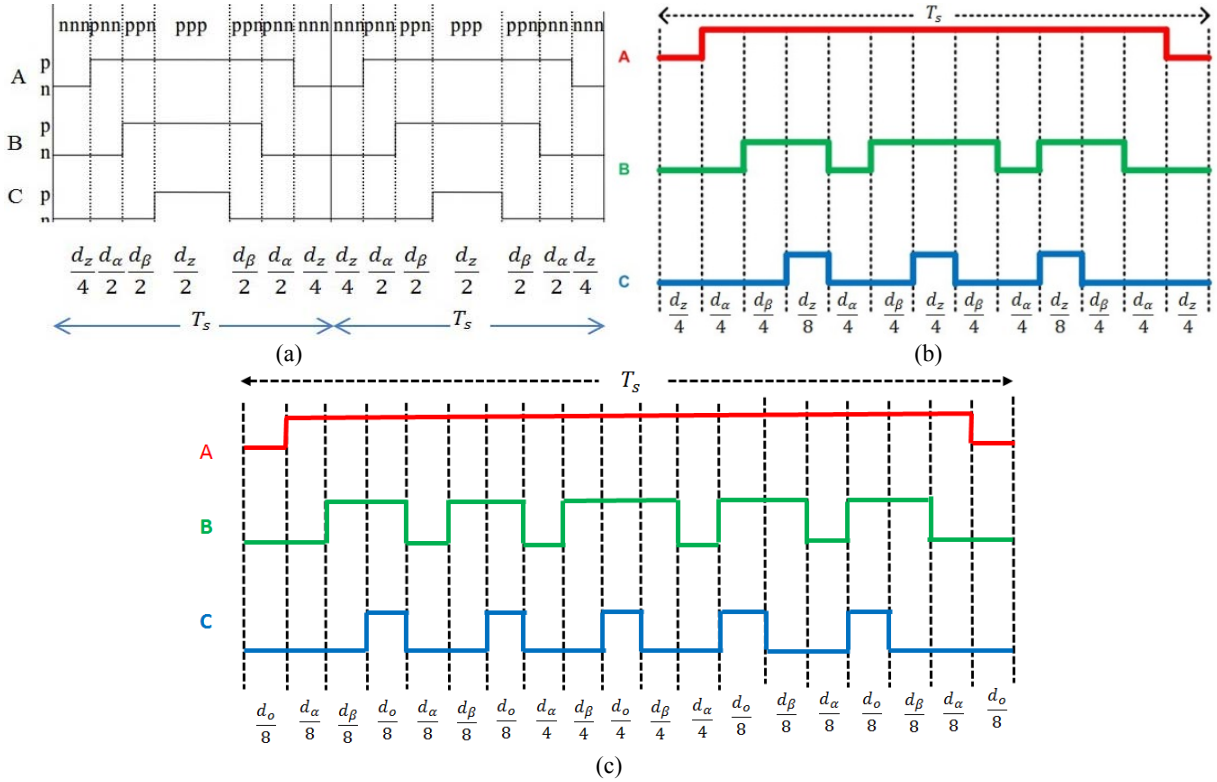

Fig. 10 (a) Conventional SSA; (b) Modified symmetric SSA; (c) Ultra-modified SSA.

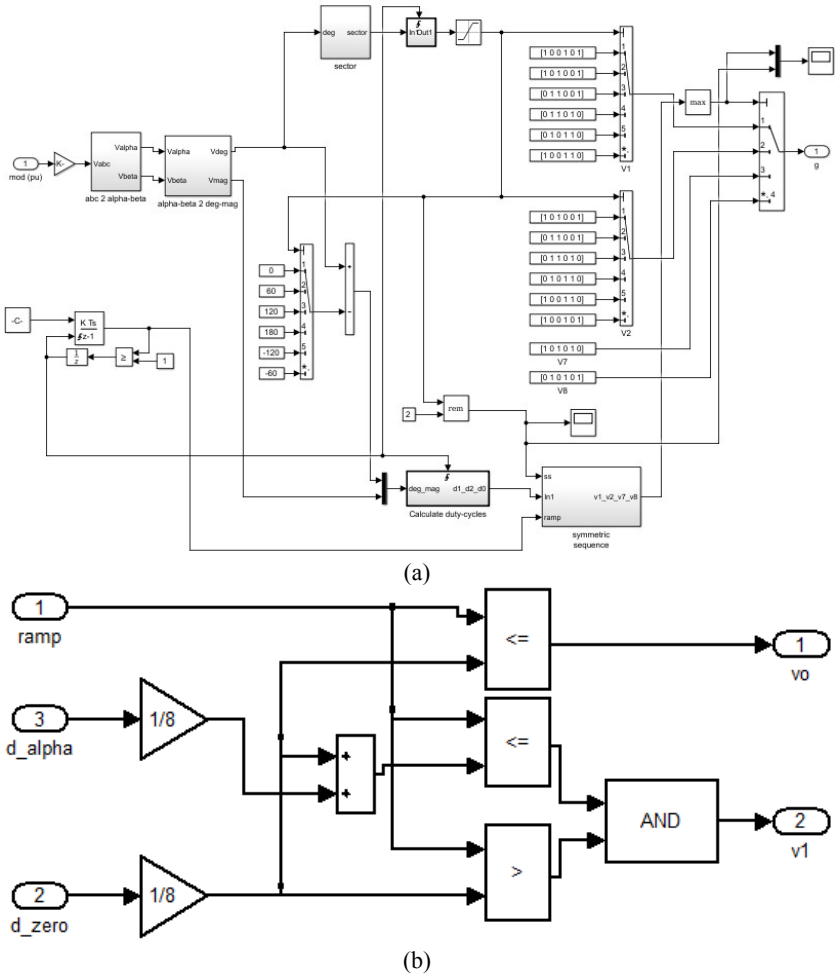

Fig. 11 Implementation of the ultra-modified SSA.

This can be achieved by comparing the one-eighty of zero vectors duty cycle with a ramp signal of a switching time equal to 2 μs as shown in Fig. 11b. Then is to apply the first vectors for a time equal to one-eighty its period. This can be achieved as shown in Fig. 11b. The third step is to apply the second vectors for a time equal to one-eighty its period and so on.

6. Modified Feed Forward Control of MC

The output voltage of MC in case of feed forward control is a percent of the input voltage. If q is the ratio between output voltage and input voltage, if q = 0.4 in feed forward control, input voltage = 200 V, the output voltage will be 80 V but with the required frequency. If the input voltage changes from 200 V to 100 V the output voltage will be 40 V. If we need to obtain constant output voltage the q ratio must be changed from 0.4 to 0.8 so the q ratio must be depend on the input voltage and this can be achieved by modified feed forward control. Modified feed forward controller takes a signal from three-phase input voltage and q ratio can be calculated as in Eq. (27). From both Table 1 and Eq. (27) the ratio q in case of modified feed forward control depends on the input voltage where if the input voltage decreased the ratio q increased so that obtain a constant output voltage. Fig. 12a shows the proposed modified feed forward control of indirect space vector modulation. Fig. 12b shows MATLAB Simulink modification in the proposed modified feed forward control of indirect space vector modulation. Fig. 12b shows that a signal of the three phase input voltages is taken in case of the modified control and this signal is converted to magnitude

Table 1 Modified feed forward control.

V_{IN}	Feed forward control		Modified feed forward	
	q	V_{out}	q	V_{out}
200	0.4	80	0.4	80
100	0.4	40	0.8	80

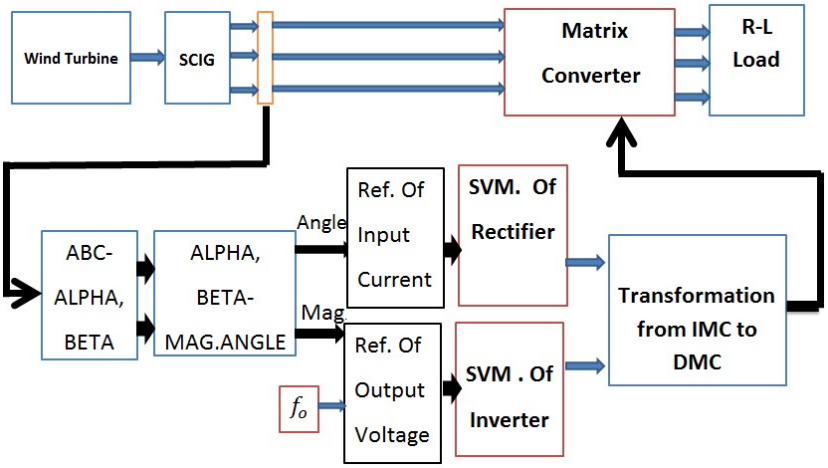

(a) Block diagram of model

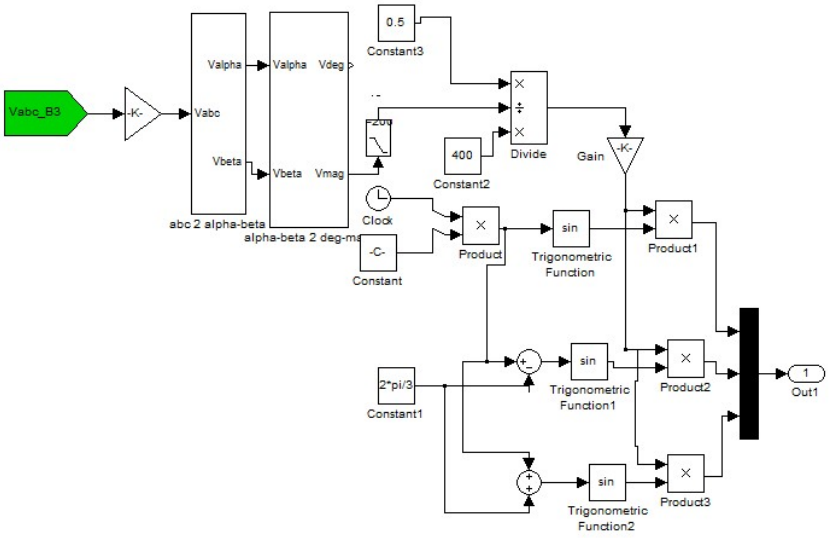

(b) Simulink of modification in the model

Fig. 12 Modified feed forward control.

and value. Then the reference or the desired value of output voltage is divided by this value to obtain the per unit reference output voltage vector. In this case the reference output voltage vector inversely proportional to the input voltage, so constant output voltage can be obtained from the modified control.

$$q = \frac{V_{out}^*}{V_{IN}} \quad (27)$$

7. Simulation Results

7.1 SSA

Simulations were done using MATLAB/Simulink for a MC interfaced 50 Hz three-phase supply with an R-L load (R = 144 Ω, L = 0.25 H). The ultra-modified is used with indirect space vector to control MC. The

modified algorithm reduces the THD for the output voltage as shown in Fig. 14 also THD for output voltage with conventional SSA is shown in Fig. 13a. The simulation results showed that the THD of output voltage is reduced with the modified algorithm. The modified method decreases the THD of the output voltage so decrease cost and size of the required filter but this a method increases THD of the output current as shown in Fig. 14b. The proposed method decreases the THD of the output voltage and current as shown in Fig. 15. The THD of the output voltage and current is shown as in Table 2. Fig. 16 shows IDF factor control, Fig. 16a shows unity IDF, Fig. 16b shows IDF with displacement factor angle equal to 20°.

Table 2 Simulation results of THD for conventional and modified SSA.

	THD of output voltage %	THD of output current %
Conventional SSA	37.91	2.14
Modified SSA	18.88	2.21
Ultra-modified SSA	15.32	1.59

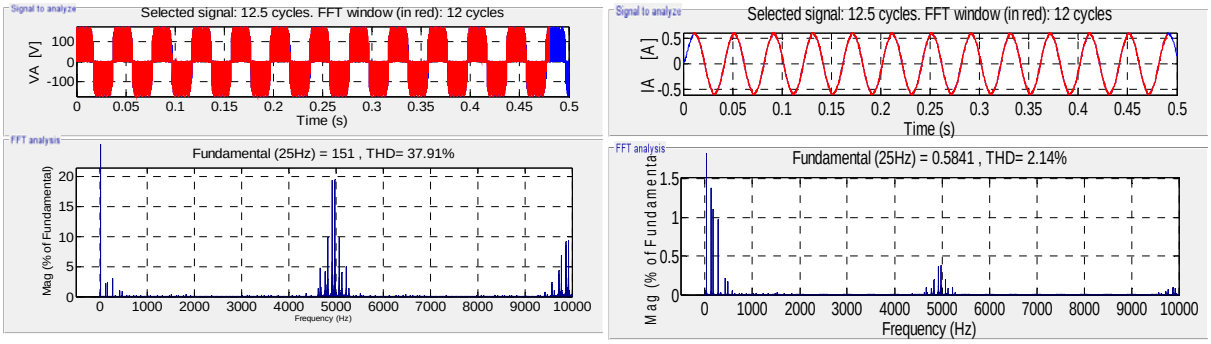

(a) (b)

Fig. 13 Simulation result of THD for 25 Hz (a) Output voltage; (b) Output current for conventional SSA.

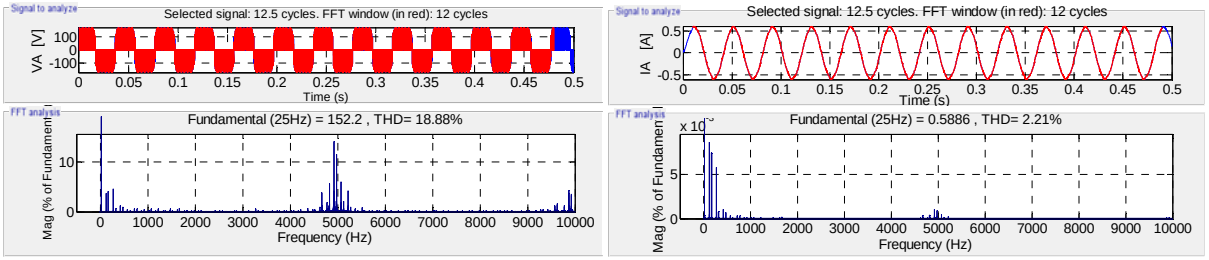

(a) (b)

Fig. 14 Simulation result of THD for 25 Hz (a) Output voltage; (b) Output current for modified SSA.

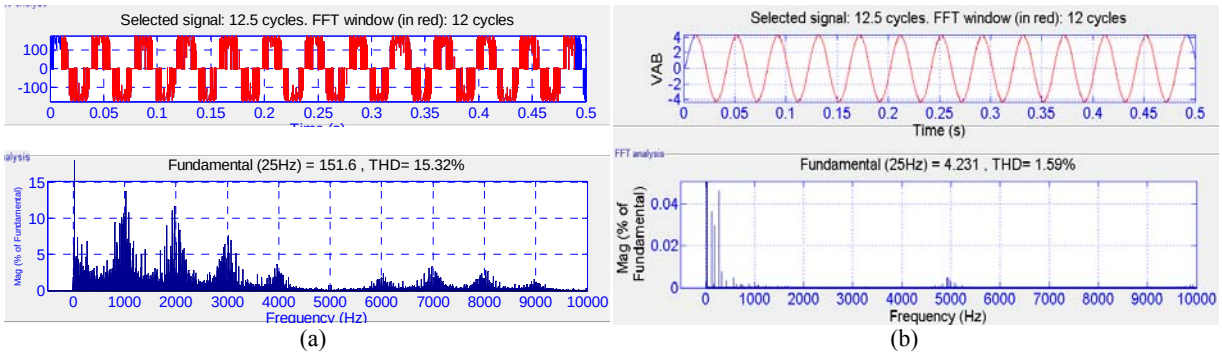

(a) (b)

Fig. 15 Simulation result of THD for 25 Hz (a) Output voltage; (b) Output current for ultra-modified SSA.

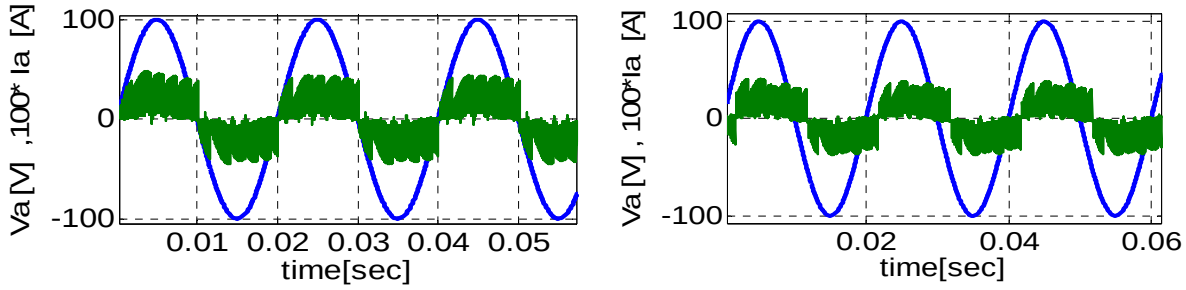

(a) Unity IDF (b) IDF of angle 20°

Fig. 16 Control of IDF.

Table 3 Variation of generated voltage and frequency with wind velocity.

Wind velocity m/s	Voltage (V)	Frequency (Hz)
6	280	21
7	320	25
9	380	34
12	460	46

7.2 Modified Feed Forward

Simulations were done using MATLAB/Simulink software package results for a MC interfaced WECS (wind energy conversion system) for R-L load (R = 2 Ω, L = 1 mH). MC is controlled by using ISVM with modified feed forward control to obtain the desired output voltage and frequency. Fig. 12 shows simulation results at different wind speed with feed forward control. Fig. 13 shows simulation results at different wind speeds with modified feed forward control. In case of a modified feed forward control the output voltage and frequency remain constant to the desired value 220 V, 50 Hz even if the wind speed changed. In case of feed forward control the output voltage is a ratio of input voltage so if the input voltage changes, the output voltage will be changed as shown in Fig. 12. Table 3 gives the magnitude of voltages and frequency with variation of wind speeds. Fig. 17a shows wind velocity with time, where the speed of wind changed from 7 m/s to 12 m/s at t = 0.3 sec, from 12 m/s to 9 m/s at t = 0.6 sec, from 9 m/s to 6 m/s at t = 1 sec. Fig. 17b shows input voltage to MC (generated voltage) and this figure shows that the input voltage change from 320 V , 25 Hz to 460 V ,46 Hz at t = 0.3 sec, then from 460 V, 46 Hz to 380 V, 34 Hz at t = 0.6 sec, then from 380 V, 34 Hz to 280 V, 21 Hz at t = 1 sec. The change in input voltage amplitude and frequency is due to the change in the wind speed that make the output voltage also change as shown in Fig. 17c. Fig. 17d shows simulation results of output current of 50 Hz with feed forward control. Fig. 18b shows input voltage to MC (generated voltage), where for t = 0:0.3 sec the generated voltage is 320 V, 25 Hz, where for t = 0.3:0.6 sec the generated voltage is 460 V, 46 Hz, where for t = 0.6:1 sec the generated voltage is 380 V, 34 Hz, where for t = 1:1.5 sec the generated voltage is 280 V, 21 Hz. Fig. 18c shows simulation results for the desired output voltage of 220 V, 50 Hz with modified feed forward control. It is clear from Fig. 18c that the magnitude of the output voltage is constant and equal to the reference value = 220 V; Fig. 18d shows simulation results of output current of 50 Hz with modified feed forward control. Table 4 and 5 show that the output voltage from MC changes with change in input voltage with the convention feed forward controller.

8. Experimental Results

8.1 SSA

Experimental results were performed using DSP1104, for a MC interfaced 50 Hz three-phase supply with an isolated R-L load (R = 144Ω, L = 0.25 H)

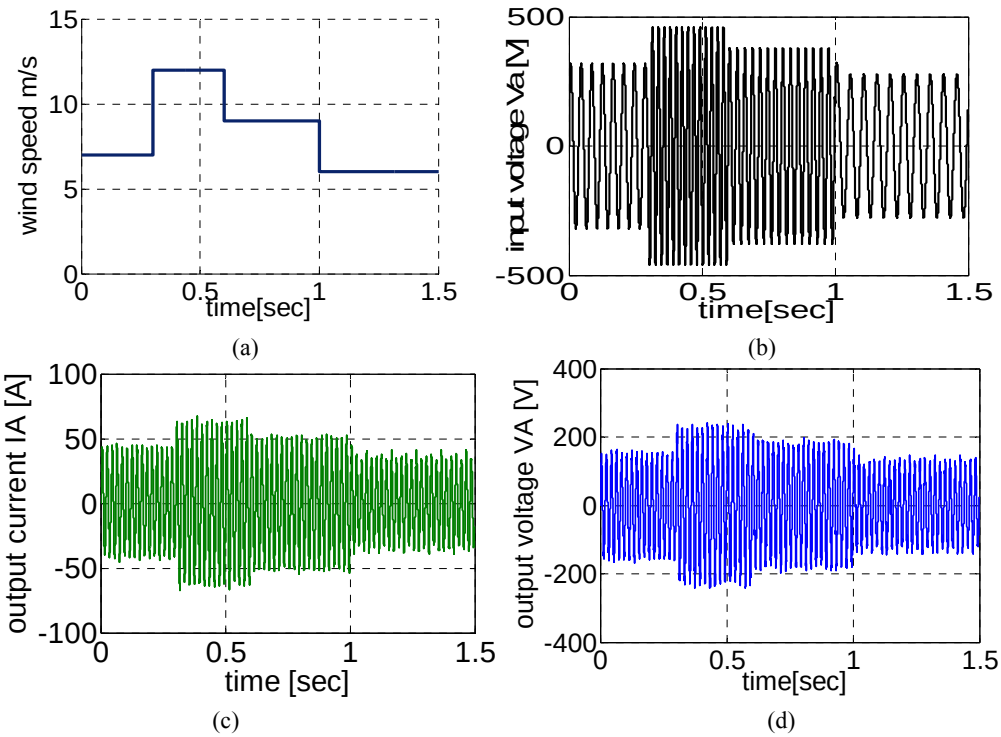

Fig. 17 Simulation results for feed forward control of MC, (a) Wind speed; (b) Input voltage V_a; (c) Output voltage V_A 50 Hz; (d) Output current I_A 50 Hz.

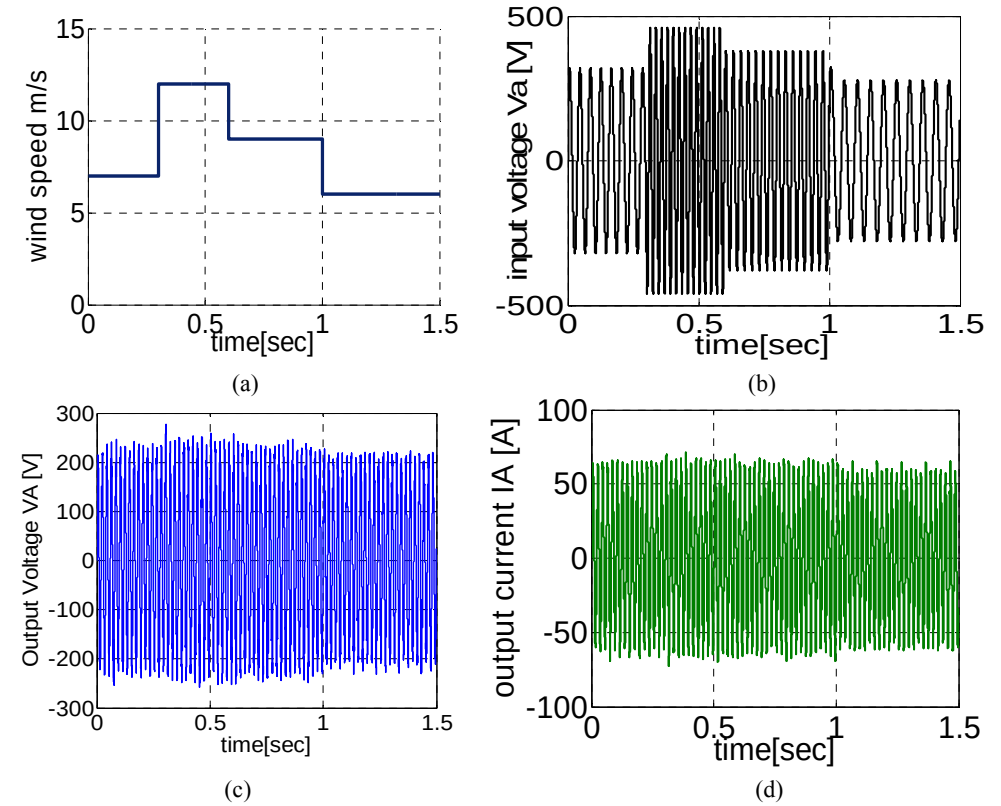

Fig. 18 Simulation results for modified feed forward control of MC, (a) Wind speed; (b) Input voltage V_a; (c) Output voltage V_A 50 Hz; (d) Output current I_A 50 Hz.

Table 4 Simulation values of the variation of output voltage and frequency from MC with feed forward.

Wind velocity m/s	Voltage (V)	Frequency (Hz)
6	140	50
7	160	50
9	190	50
12	230	50

Table 5 Simulation values of the variation of output voltage and frequency from MC with the modified feed forward.

Wind velocity m/s	Voltage (V)	Frequency (Hz)
6	220	50
7	220	50
9	220	50
12	220	50

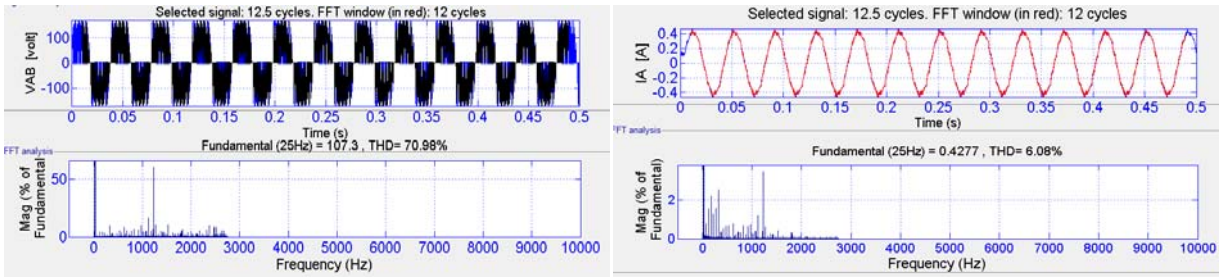

(a) (b)

Fig. 19 Experimental results forTHD for 25 Hz, (a) Output voltage; (b) Output current for conventional SSA.

that will be presented with switching time = 0.0002 sec. The experimental results showed that the THD of output voltage is reduced with the modified algorithm and ultra modified algorithms where Fig. 19 shows THD for output voltage and current with conventional algorithm, Fig. 20 shows the THD with modified algorithm and Fig. 21 shows experimental results for output voltage and current with the proposed algorithm which have the lower Value for THD. The THD of the output voltage and current is shown as in Table 6.

8.2 Modified Feed Forward

Experimental results were performed using DSP1104, with an isolated static load of (R = 20 Ω, L = 40 mH). The field and armature voltage of DC motor are controlled to control its speed to simulate WT. Fig. 22 shows experimental results for change in speed at a time 20 sec in case of feed forward control with 50 Hz output frequency, where Fig. 22a shows the change in speed where speed changes from 1,535 rpm to 1,675 rpm by increasing the armature voltage. Fig. 22b shows the input voltage where the rms value and frequency of the input voltage increase with the increase in speed. Fig. 22c shows output voltage in case of feed forward control and Fig. 22d shows zoomed view of output voltage which has 50 Hz frequency. The output frequency does not change even if the input frequency changes. The rms value of the output voltage is a percent of the input voltage so the rms value of the output voltage changes with change in input voltage as in Fig. 22d. The change in output voltage is due to the q ratio (ratio between output voltage and input voltage) which is fixed in conventional feed forward control. In modified feed forward control q ratio is calculated from input voltage and the reference output voltage so if the input voltage decreases the q ratio is increased by the modified control, so that a constant output voltage can be achieved as shown in Fig. 23. Fig. 23 shows the experimental results for change in speed at a time 18.5 sec in case of modified feed forward control with 50

Hz output frequency, where Fig. 23a shows the change in speed where speed changes from 1,528 rpm to 1,653 rpm by increasing the armature voltage. Due to the change in speed the input voltage magnitude and input frequency increase from 29.3 Hz to 33.5 Hz approximately as shown in Fig. 23b. In case of modified control the q ratio will be changed inversely with the change in input voltage so that a constant

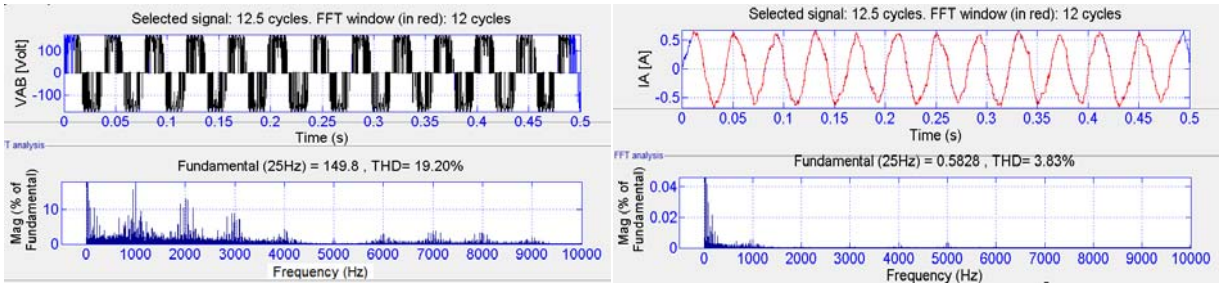

(a) (b)

Fig. 20 Experimental results for THD for 25 Hz, (a) Output voltage; (b) Output current for modified SSA.

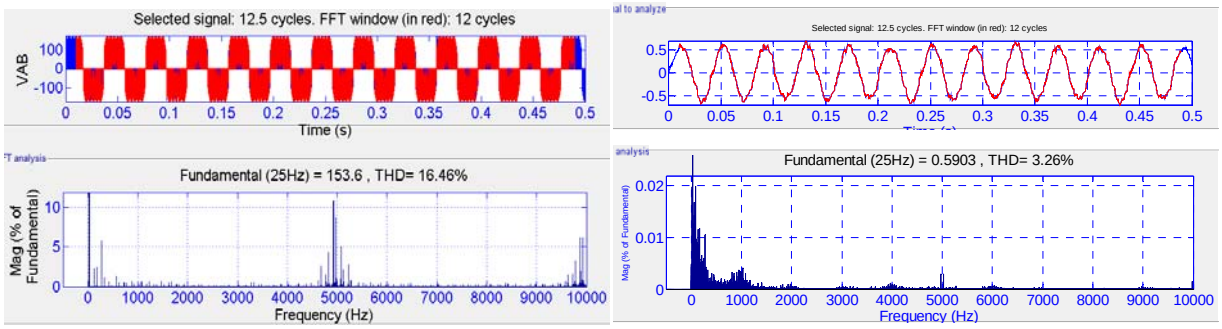

(a) (b)

Fig. 21 Experimental results for THD for 25 Hz, (a) Output voltage; (b) Output current for ultra-modified SSA.

Table 6 Experimental result of THD for conventional, modified and ultra-modified SSA.

	THD of output voltage %	THD of output current %
Conventional SSA	70.98	6.08
Modified SSA	19.2	3.83
Ultra-modified SSA	16.46	3.26

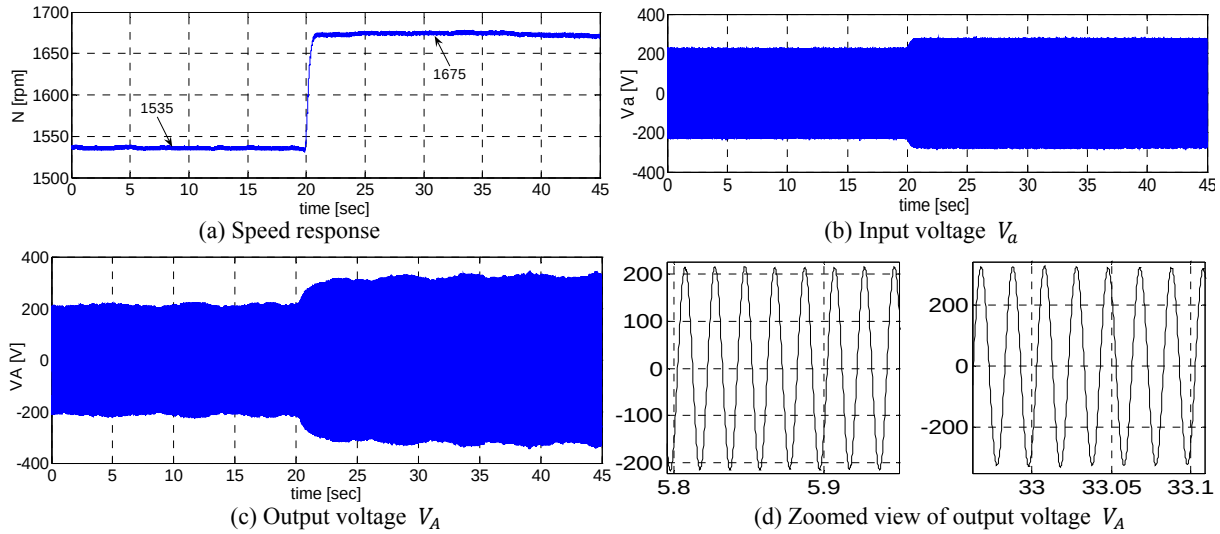

(a) Speed response (b) Input voltage V_a

(c) Output voltage V_A (d) Zoomed view of output voltage V_A

Fig. 22 Experimental results with open loop control & output frequency 50 Hz.

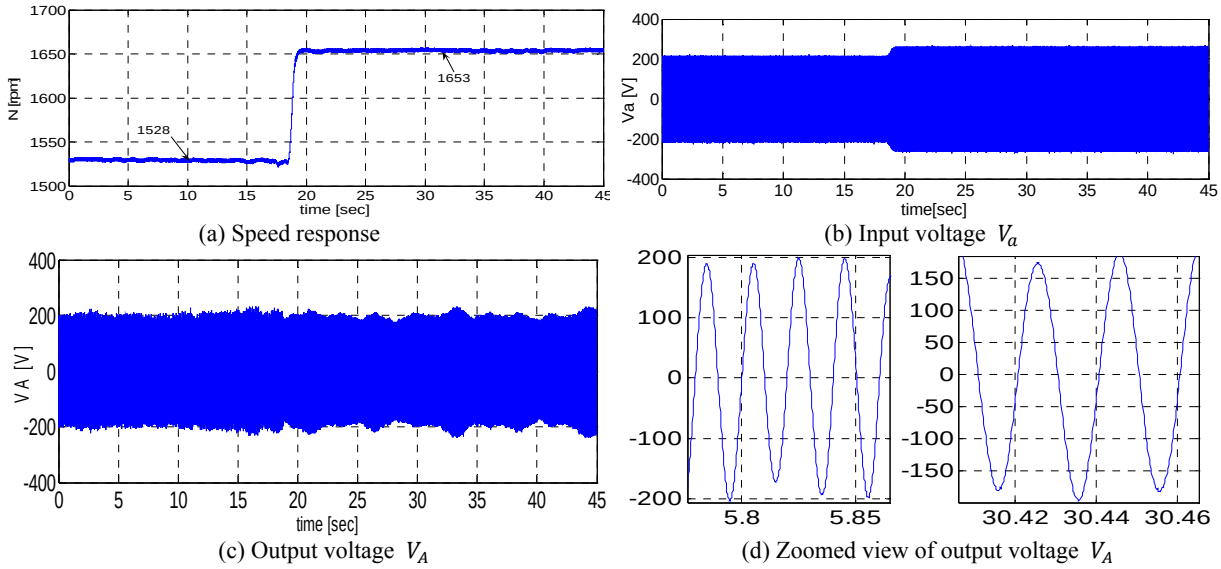

Fig. 23 Experimental results with modified feed forward control & output frequency 50Hz.

output voltage can be achieved as shown in Fig. 23c. Fig. 23d shows zoomed view of output voltage which has a frequency of 50 Hz. The output frequency does not change even if the input frequency changes. The rms value of the output voltage is a percent of the input voltage.

9. Conclusions

In this paper, an ultra-modified SSA of space vector modulation of MC is introduced which overcomes the drawbacks of the modified algorithm, where it reduces both THD of output voltage and current. The angle between input voltage and input current of MC can be controlled and unity IDF is achieved. In addition to a modified feed forward controller for the ISVM used in MC (MC) was introduced. This controller improves the performance of MC with variable speed WT operation. The voltage and frequency of a static R-L load can be controlled by using a MC fed from WECS. The proposed modification in the feed forward controller of MC gives a solution for the change in the output voltage magnitude due to change in wind speeds. The analysis of ISVM was introduced, in addition to introducing how to transform from indirect MC to direct one. An experimental setup for MC with modified feed forward controller was introduced. The simulation and experimental set up results are consistent with the expected results.

References

[1] Aydogmus, O., and Deniz, E. 2017. "Design and Implementation of Two-Phase Permanent Magnet Synchronous Motor Fed by a MC." *IET Power Electronics* 10: 1054-60.

[2] Wang, L., Dan, H., Zhao, Y., Zhu, Q., Peng, T., Sun, Y., et al. 2018. "A Finite Control Set Model Predictive Control Method for MC with Zero Common-Mode Voltage." *IEEE Journal of Emerging and Selected Topics in Power Electronics* 6 (1): 327-38.

[3] Prasad, P. S., Kumar, A. B. V. S., and Rao, G. S. 2016. "Induction Motor Speed Control by Carrier Modulation Based MC." In *Proceedings of the 2016 International Conference on Signal Processing, Communication, Power and Embedded System (SCOPES)*, 1176-80.

[4] Luo, F. L., and Pan, Z. Y. 2006. "Sub-envelope Modulation Method to Reduce Total Harmonic Distortion of AC/AC MCs." In *Proceedings of the 2006 37th IEEE Power Electronics Specialists Conference*, 1-6.

[5] Gyugyi, L., and Pelly, B. R. 1976. *Static Power Frequency Changers: Theory, Performance, and App1ication.* IEEE Trans. Antennas Propagat.

[6] Venturini, M., and Alesina, A. 1980. "The Generalised Transformer: A New Bidirectional, Sinusoidal Waveform Frequency Converter with Continuously Adjustable Input Power Factor." In *Proceedings of the 1980 IEEE Power Electronics Specialists Conference*, 242-52.

[7] Xiao, D., and Rahman, M. F. 2006. "A Modified Direct Torque Control for a MC-Fed Interior Permanent Magnet Synchronous Machine Drive." In *Proceedings of the 2006 37th IEEE Power Electronics Specialists Conference*, 1-7.

[8] Wang, B., and Sherif, E. 2013. "Spectral Analysis of MCs Based on 3-D Fourier Integral." *IEEE Transactions on Power Electronics* 28: 19-25.

[9] Saha, J., Ayad, A., and Kennel, R. 2017. "Direct Model Predictive Current Control for MCs." In *Proceedings of the 2017 International Conference on Nascent Technologies in Engineering (ICNTE)*, 1-5.

[10] Moftah, M. A. M. A., Taha, G. E. S. A., and Ibrahim, E. N. A. 2016. "Active Power Filter for Variable-Speed WT PMSG Interfaced to Grid and Non-linear Load via Three Phase MC." In *Proceedings of the 2016 Eighteenth International Middle East Power Systems Conference (MEPCON),* 1013-9.

[11] Dabour, S. M., and Rashad, E. M. 2012. "Analysis and Implementation of Space-Vector-Modulated Three-Phase MC." *IET Power Electronics* 5: 1374-8.

[12] Dabour, S. M., Allam, S. M., and Rashad, E. M. 2015. "Indirect Space-Vector PWM Technique for Three to Nine Phase MCs." In *Proceedings of the 2015 IEEE 8th GCC Conference & Exhibition*, 1-6.

[13] Tawfiq, K. B., Abdou, A. F., El-Kholy, E. E., and Shokrall, S. S. 2016. "Application of MC Connected to Wind Energy System." In *Proceedings of the 2016 Eighteenth International Middle East Power Systems Conference (MEPCON)*, 604-9.

[14] Tawfiq, K. B., Abdou, A. F., El-Kholy, E. E., and Shokralla, S. S. 2016. "A Modified Space Vector Modulation Algorithm for a MC with Lower Total Harmonic Distortion." In *Proceedings of the 2016 IEEE 59th International Midwest Symposium on Circuits and Systems (MWSCAS)*, 1-4.

[15] Amin, A. A., Tawfiq, K. B., Youssef, H., and El-Kholy, E. E. 2016. "Performance Analysis of Inverter Fed from Wind Energy System." In *Proceedings of the 2016 Eighteenth International Middle East Power Systems Conference (MEPCON)*, 512-6.